Honeycomb hexagon pattern in dielectric barrier discharge

Lifang Dong,* Weili Liu, Hongfang Wang, Yafeng He, Weili Fan, and Ruiling Gao
College of Physics Science & Technology, Hebei University, Baoding, 071002, China
(Received 23 March 2007; revised manuscript received 20 July 2007; published 10 October 2007)

We report on a honeycomb hexagon pattern in dielectric barrier discharge. It bifurcates from a square pattern as the applied voltage is increased. A phase diagram of the pattern types as a function of the gas component and applied voltage is presented. The spatial Fourier spectrum of the honeycomb hexagon pattern is a hexagonal superstructure with three wave vectors $\vec{k}_1^h$, $\vec{k}_2^s$ and $\vec{k}_3^s$ at least, demonstrating that the pattern is a superlattice pattern. Measurements of the correlation between discharge filaments indicate that the honeycomb hexagon pattern is an interleaving of three different transient hexagonal sublattices, whose spatial wave vectors are exactly equal to $\vec{k}_1^h$, $\vec{k}_2^s$ and $\vec{k}_3^s$, respectively. These three wave modes fulfill a triad resonance condition $\vec{k}_3^s - \vec{k}_2^s = \vec{k}_1^h$.

DOI: 10.1103/PhysRevE.76.046210 PACS number(s): 89.75.Kd, 47.54.−r, 52.80.Tn

The pattern with six fold symmetry is a subject of widespread interest in many nonlinear systems. Especially, several kinds of hexagon patterns with honeycomb structures have been observed in Faraday systems, reaction-diffusion systems, and nonlinear optical systems [1–5]. In Faraday experiments, a cell of this kind of pattern consists of a honeycomb with solid lines and a spot inside. Generally, it is a single oscillated primary hexagon pattern. For example, it is a hexagon pattern oscillated subharmonically in the silicone oil fluid driven by single-frequency forcing [1]. A similar hexagon pattern generated by single-frequency acceleration in a viscoelastic liquid is a harmonic one [2]. With two-frequency forcing in Newtonian liquid, the temporal response of a hexagon pattern is subharmonic [3]. In a photosensitive reaction-diffusion system, it is a superlattice honeycomb structure containing continuous white and black lines corresponding to the concentrations of different complexes, respectively [4]. A regular honeycomb pattern is observed in the far field in the nonlinear optical system, which shows a hexagonal array of solid luminous areas [5]. In this paper, we report a honeycomb hexagon pattern whose cell is composed of spots in a dielectric barrier discharge.

Dielectric barrier discharge (DBD) is a kind of nonequilibrium gas discharge, which has been well known for its industrial applications such as ozone generation and plasma display panels [6]. In recent years, the DBD system has become an attractive pattern formation system since a variety of patterns have been observed [7–16]. Depending on the product of gas pressure and gas gap width, the discharge operates in different regimes. When the product is more than several tens of Torr cm, the discharge consists of many filaments. These filaments can self-organize into various types of regular patterns for different parameters.

In this paper, the appearance of honeycomb hexagon patterns as a function of the gas component and applied voltage is studied. The spatiotemporal dynamics of the honeycomb hexagon pattern is studied by an optical method. It is proved that the honeycomb hexagon pattern is an interleaving of three transient hexagonal sublattices. It is a superlattice pattern resulting from a triad resonant interaction.

Details of the experimental apparatus were described previously [10]. The following is a brief description. Two cylindrical containers with diameter of 75 mm, sealed with 1.5-mm-thick glass plates, are filled with water. A metallic ring immerses in the water in each container and is connected to a power supply. Thus, the water acts as a liquid electrode and the glass plates serve as dielectric layers. A glass frame with a thickness of 1.5 mm is placed between the two parallel glass plates, serving as the lateral boundary. A sinusoidal ac voltage is applied to the electrodes. The driving frequency can vary from 30 kHz to 65 kHz. All of the apparatus is enclosed in a large container filled with the mixture of argon and air at 1 atm pressure. The argon component is from 99.1% to 99.9%. The amplitude of the applied voltage is measured by a high-voltage probe (Tektronix P6015A, 1000×) . The light emitted from different discharge filaments is detected by two lens-aperture photomultiplier tube (PMTs, RCA 7265) systems and recorded by an oscilloscope (Tektronix TDS3054B, 500 MHz) simultaneously. Thus, the correlation between two filaments can be studied.

The honeycomb hexagon pattern can be observed under boundaries with different shapes, such as a square, circle, and hexagon, as shown in Fig. 1. In this paper, we will focus on the honeycomb hexagon pattern with hexagonal boundaries as the pattern is more regular than others. In addition, a square superlattice and a hexagon superlattice pattern can also be observed with the square and circular boundaries under other experimental conditions [13,14].

Figure 2 presents a bifurcation scenario of the discharge pattern as the applied voltage increasing continuously, as follows: random filaments–square pattern-coexistence of squares and honeycomb cells-honeycomb hexagon pattern-chaos state. A few filaments appear when the driving voltage reaches the breakdown voltage. The number of filaments increases with the voltage and the filaments arrange randomly as shown in Fig. 2(a). After filaments form a regular square pattern as shown in Fig. 2(b), some imperfect honeycomb cells invade the square domain, as shown in Fig. 2(c). The honeycomb cells grow gradually and cover the whole discharge area with the voltage increased. As a result, a global hexagon pattern with perfect honeycomb cells forms, as

*Donglf@mail.hbu.edu.cn

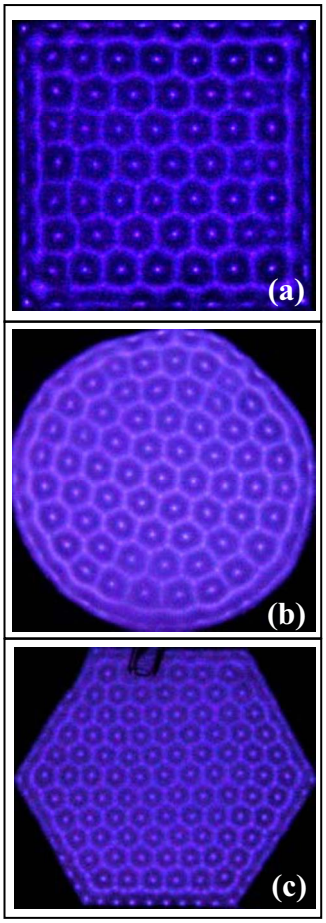

FIG. 1. (Color online) The honeycomb hexagon patterns observed in the DBD system with different boundaries: (a) square boundary, (b) circular boundary, and (c) hexagonal boundary.

shown in Fig. 2(d). With the voltage increasing, the honeycomb pattern with more cells emerges, as shown in Fig. 2(e). A further increase in voltage leads to a chaos state, as shown in Fig. 2(f). Obviously, no a sudden replacement by a distinct state has been observed; for example, a transition state is observed in the bifurcation from the square pattern to global honeycomb hexagon pattern. Therefore, the observed transitions between different patterns are smooth or continuous.

A phase diagram of the pattern types as a function of argon concentration χ and applied voltage U is presented in Fig. 3. It is obtained by increasing the applied voltage from 0 to about 10 kV at several constant argon concentrations and a fixed frequency 56 kHz. A transition voltage boundary is defined when a new spatiotemporal structure appears or an existing one dies out. Based on data from repetitious experimental runs, the statistical mean values of boundary voltages are used for the phase diagram and the corresponding error is about 100 V. Specially, just a region where global honeycomb patterns with a perfect structure exist is described as the phase region of honeycomb hexagon pattern. It is found that a honeycomb hexagon pattern emerges over a range of argon concentration from 99.4% to 99.9% approximately.

Figure 4 exhibits the spatial Fourier spectrum of the honeycomb hexagon pattern image with high contrast. From Fig.

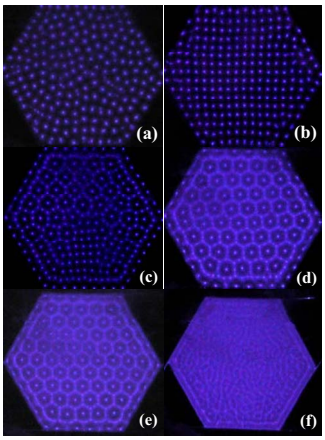

FIG. 2. (Color online) The bifurcation scenario of patterns as the applied voltage U increasing. (a) Filaments with random arrangement, $U=3.0$ kV. (b) Square pattern, $U=3.5$ kV. (c) Coexistence of squares and honeycomb cells, $U=3.6$ kV. (d) Honeycomb hexagon pattern, $U=3.7$ kV. (e) Honeycomb hexagon pattern whose cell is smaller than that in (d), $U=3.9$ kV. (f) Chaos state, $U=4.7$ kV. The exposure time of photographs is 40 ms. The component of argon is about 99.9%. The incircle diameter of hexagonal boundary is 100 mm. The other parameters are the gas pressure $p=760$ Torr, gas gap $d=1.5$ mm, and driving frequency $f=56$ kHz.

4(a), it can be clearly seen that each honeycomb cell is composed of several individual spots (filaments), which is different from the lines composing the honeycomb cell in other systems mentioned above. In Fig. 4(b), the Fourier spectrum exhibits a hexagonal superstructure with three wave numbers at least, indicating that the honeycomb hexagon pattern should be a superlattice. The difference from the spectrum of the hexagon pattern observed in Faraday system is the existence of $\vec{K}=2\vec{k}_2$ besides the two inner hexagonal lattices [1].

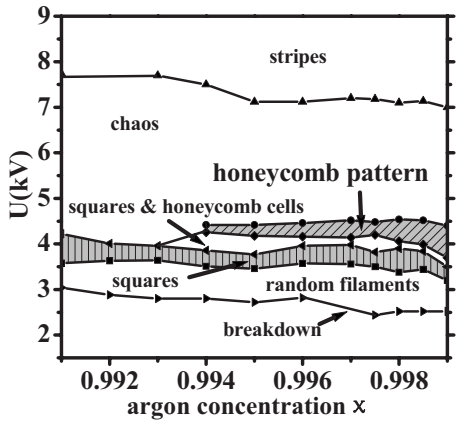

FIG. 3. Phase diagram of the observed patterns obtained by quasistatically increasing the driving voltage U at a series of certain argon concentrations x. The symbols mark the observed transition points between different patterns; the lines are guides for the eyes. The regions of square pattern, a coexistence of squares and honeycomb cells, honeycomb hexagon pattern, chaos, and stripes are indicated, respectively. The bottom line represents the threshold voltages for breakdown. The driving frequency is 56 kHz.

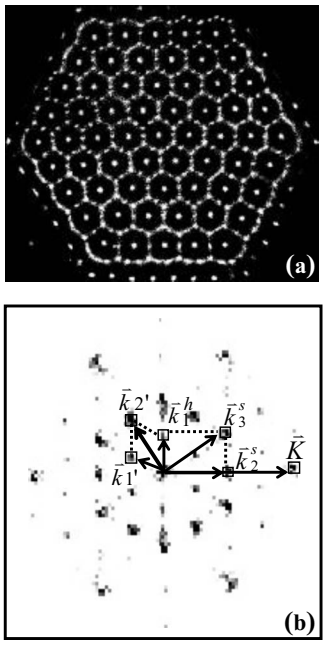

FIG. 4. A high-contrast image of honeycomb hexagon pattern and the corresponding spatial Fourier spectrum. One of the possible spatial resonances is $\vec{k}_1+\vec{k}_2=\vec{k}_3$. The superscript s (h) denotes subharmonic (harmonic) response to the applied voltage.

As is well known, a simple hexagonal lattice is formed by a resonant triplet of vectors with equal wave number. The Fourier spectrum shows that the pattern contains several such triplets with shifts in phase between $\vec{k}_2^s$ and $\vec{k}_1^h$ or $\vec{k}_3^s$. Several possible resonances are present in the Fourier spectrum, such as $\vec{k}_1+\vec{k}_2=\vec{k}_3$, $\vec{k}_1+\vec{k}_1'=\vec{k}_2'$, and so on, in which the most reasonable one will be discussed later.

In order to study the spatiotemporal dynamics of the honeycomb hexagon pattern, a series of temporal correlation measurements are conducted. At first, the light emission of individual filaments located at the center, the vertex, and the side of any honeycomb cells, which are denoted by A, B, and C, respectively, in Fig. 5(a), are measured and shown in Fig. 5(b) and 5(c). And for comparison the light emission from the total pattern is detected simultaneously. It is clearly seen that the light emission from the total pattern has three discharge pulses per half cycle of the voltage and the light emission from any individual filament has one pulse which corresponds to different pulses of the total light signal. So the honeycomb hexagon pattern should consist of several substructures discharging nonsynchronously. Obviously, filament A discharges harmonically with respect to the driven period of light emission as the same interval between two pulses in consecutive half cycles. Filaments B and C discharge subharmonically because the intervals of two discharge pulses in consecutive half cycles are alternating between a long one and a short one. (Note that the driven period is the half cycle of the applied voltage because the light emission is independent of the sign of the voltage.)

Then the correlation between two individual filaments from one honeycomb cell and from different cells is measured and shown in Fig. 6. The measurements from one honeycomb cell are presented in Figs. 6(a)–6(c). Two filaments with different locations discharge nonsynchronally in each half cycle of the voltage [see Figs. 6(a) and 6(b)]. And the filaments with the same locations discharge simultaneously [see Fig. 6(c)]. Similar results for the filaments from different cells selected randomly are exhibited in Figs. 6(d)–6(f). So all filaments located at the centers of any honeycomb cells volley and compose one hexagonal sublattice. It is the

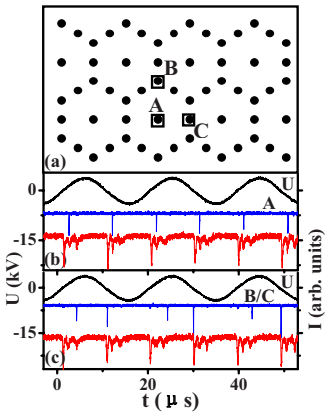

FIG. 5. (Color online) The light signal of single filament located at different positions of any honeycomb cell, which are denoted by different letters in (a). (b) The light signal (middle curve) of any filament A located at the center of a honeycomb cell. (c) The light signal (middle curve) of any filament B located at the vertex of a honeycomb cell. The light signal of any filament C located at the side of a honeycomb cell is similar to (b). In (b) and (c), the wave forms of applied voltage U (upper curves) and the light signals of total pattern (bottom curves) are presented.

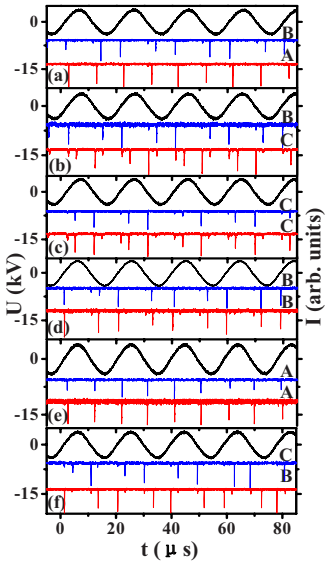

FIG. 6. (Color online) The temporal correlation between the light signals of different filaments. The light signals of (a) B and A, (b) B and C, and (c) two filaments C in the same honeycomb cell. The light signals of (d) two filaments B, (e) two filaments A, and (f) C and B in different honeycomb cells selected randomly. In each graph, the top wave form is the applied voltage.

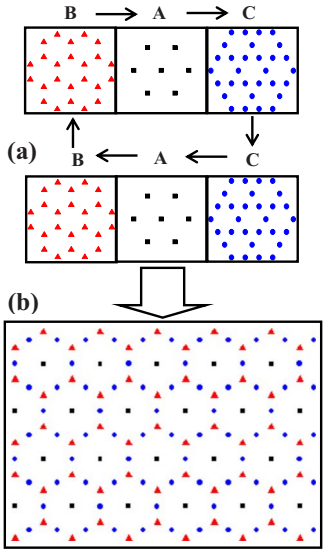

FIG. 7. (Color online) Schematic diagram of (a) spatiotemporal evolution of the honeycomb hexagon pattern in one cycle of the applied voltage and (b) a time integral of (a). The three sublattices are denoted by different symbols. The arrows in (a) indicate the time sequence.

same case for all the filaments located at the vertexes and the sides of any cells. From these results, it can be concluded that the honeycomb hexagon pattern is an interleaving of three hexagonal sublattices composed of filaments *A*, *B*, and *C*, respectively, whose schematic diagram is given in Fig. 7. The discharge sequence of these sublattices in one cycle of the applied voltage is *B*-*A*-*C*-*C*-*A*-*B* as shown in Fig. 7(a). Sublattice *A* exhibits a harmonic response, while sublattices *B* and *C* exhibit the subharmonic response. So it is a mixed oscillated pattern. Obviously, the spatial wave vectors of these three sublattices *A*, *B*, and *C* are exactly equal to $\vec{k}_1^h$, $\vec{k}_2^s$ and $\vec{k}_3^s$ in Fig. 7(b), respectively. So the $\vec{k}_1^h$ is a harmonic mode, while the $\vec{k}_2^s$ and $\vec{k}_3^s$ are subharmonic modes.

Back to the problem of the most reasonable triad resonance mentioned above, as is well known, the parity of the wave vector plays a key role in the triad resonance. Two modes of like parity can couple quadratically to a harmonic mode, but not a subharmonic mode [17]. As $\vec{k}_3^s - \vec{k}_2^s = \vec{k}_1^h$ is the only triad resonance satisfying the rule above, it is the most reasonable one among all the possible resonances.

In conclusion, a honeycomb hexagon pattern is observed in dielectric barrier discharge. This kind of hexagon pattern is a superlattice pattern, whose spatial Fourier spectrum exhibits a hexagonal superstructure with three wave numbers at least. It can be observed over a range of argon concentration from 99.4% to 99.9% approximately. The dynamics of this pattern is explored by conducting a series of spatiotemporal measurements. It is found that the honeycomb hexagon pattern is an interleaving of three transient hexagonal sublattices. These sublattices discharge harmonically or subharmonically, and their spatial wave modes are $\vec{k}_1^h$, $\vec{k}_2^s$, and $\vec{k}_3^s$ in the Fourier spectrum, respectively. These three wave modes fulfill a reasonable triad resonance interaction $\vec{k}_3^s - \vec{k}_2^s = \vec{k}_1^h$.

This work is supported by the National Natural Science Foundation of China under Grants No. 10775037 and No. 10575027, the Specialized Research Fund for the Doctoral Program of Higher Education of China (Grant No. 20050075001), and the Natural Science Foundation of Hebei Province, China, under Grants No. A2006000950 and No. A2004000086.

[1] A. Kudrolli and J. P. Gollub, Physica D **97**, 133 (1996).
[2] C. Wagner, H. W. Müller, and K. Knorr, Phys. Rev. Lett. **83**, 308 (1999).
[3] H. W. Müller, Phys. Rev. Lett. **71**, 3287 (1993).
[4] I. Berenstein, L. F. Yang, M. Dolnik, A. M. Zhabotinsky, and I. R. Epstein, Phys. Rev. Lett. **91**, 058302 (2003).
[5] R. S. Bennink, V. Wong, A. M. Marino, D. L. Aronstein, R. W. Boyd, C. R. Stroud, Jr., S. Lukishova, and D. J. Gauthier, Phys. Rev. Lett. **88**, 113901 (2002).
[6] B. Eliasson and U. Kogelschatz, IEEE Trans. Plasma Sci. **19**, 1063 (1991).
[7] Yu. A. Astrov, I. Müller, E. Ammelt, and H.-G. Purwins, Phys. Rev. Lett. **80**, 5341 (1998).
[8] W. Breazeal, K. M. Flynn, and E. G. Gwinn, Phys. Rev. E **52**, 1503 (1995).
[9] L. F. Dong, Z. G. Mao, Z. Q. Yin, and J. X. Ran, Appl. Phys. Lett. **84**, 5142 (2004).
[10] L. F. Dong, Z. Q. Yin, X. C. Li, and L. Wang, Plasma Sources Sci. Technol. **12**, 308 (2003).
[11] L. F. Dong, Z. Q. Yin, X. C. Li, Z. F. Chai, and Y. F. He, Plasma Sources Sci. Technol. **15**, 840 (2006).
[12] L. F. Dong, F. C. Liu, S. H. Liu, Y. F. He, and W. L. Fan, Phys. Rev. E **72**, 046215 (2005).
[13] L. F. Dong, W. L. Fan, Y. F. He, F. C. Liu, S. F. Li, R. L. Gao, and L. Wang, Phys. Rev. E **73**, 066206 (2006).
[14] L. F. Dong, R. L. Gao, Y. F. He, W. L. Fan, and W. L. Liu, Phys. Rev. E **74**, 057202 (2006).
[15] L. F. Dong, Y. F. He, W. L. Liu, R. L. Gao, H. F. Wang, and H. T. Zhao, Appl. Phys. Lett. **90**, 031504 (2007).
[16] L. F. Dong, Z. Q. Yin, L. Wang, G. S. Fu, Y. F. He, Z. F. Chai, and X. C. Li, Thin Solid Films **435**, 120 (2003).
[17] H. Arbell and J. Fineberg, Phys. Rev. E **65**, 036224 (2002).